Ground-state energy of a hard-sphere Fermi fluid. II. Spin and isospin

L. P. Benofy, J. L. Gammel, and R. M. Delaney
Physics Department, St. Louis University, St. Louis, Missouri 63103

George A. Baker, Jr.
Theoretical Division, Los Alamos National Laboratory, University of California, Los Alamos, New Mexico 87545
(Received 8 July 1993)

We evaluate the fourth-order Hugenholtz diagrams from the Rayleigh-Schrödinger many-body perturbation series for a repulsive, square-well potential. We consider a system containing four different equal-mass identically interacting particle species, similar to nuclear matter when only the repulsive core is considered. We use the results of these calculations to extend the L expansion of the ground-state energy of a Fermi fluid by one more term. From this extension, we are able to provide accurate values of the ground-state energy over a density range which includes that for infinite nuclear matter.

PACS number(s): 21.65.+f, 05.30.Fk, 67.40.Db, 67.57.−z

I. INTRODUCTION AND SUMMARY

A fundamental question that has long interested physicists is the direct computation of the ground-state energy of an interacting many-fermion system. In the case of the ground state of infinite nuclear matter, the problem is complicated by uncertainty concerning the internucleon interaction potential or even the appropriateness of this description of the problem. Leaving these uncertainties aside, there is the simpler problem of the computation of the ground-state energy of a many-body system with a specified interparticle interaction. For potentials that are approximately correct for nuclear matter and helium three, there has been extensive study made [1–19] using the method of quantum thermodynamic perturbation theory. Reference [11] is hereinafter referred to as I. Satisfactory results are in hand for the case of neutron matter [14], but for the case of nuclear matter [18] the situation still needs improvement. It has become increasingly clear throughout the above-mentioned studies that in order to obtain adequate accuracy in the quantum thermodynamic perturbation, more input on the behavior of the ground-state energy of the simple repulsive-core problem is necessary. A beginning was made in this direction through the introduction of the L expansion [11] and it has been carried forward to a reasonable extent. The results were good for the case of two-particle species (such as neutron matter or He^3), but owing to fewer results in the case of four-particle species (such as nuclear matter) the results were less good.

It is the purpose of this paper to compute the series coefficients necessary to add one more term to the L-expansion of the ground-state energy of the hard-sphere, quantum, fermion fluid for the case of four-particle species. The necessary coefficients are the fourth-order Hugenholtz diagrams from the Rayleigh-Schrödinger perturbation series for the repulsive, square-well potential. A further purpose is to exploit these results to estimate the ground-state energy, through the use of the derived L expansion, for the hard-sphere Fermi fluid.

TABLE I. Arguments of the potentials and the denominators for the diagrams of classes I and I A.

Diagram	x_2	x_3	x_4	x_5	D_2	D_3
I.1	$\lvert\mathbf{q}-\mathbf{q}_1\rvert$	$\lvert\mathbf{q}_1-\mathbf{q}_2\rvert$	$\mathbf{q}_2$	$\lvert\mathbf{n}-\mathbf{m}-\mathbf{q}_2\rvert$	$q_1^2+\mathbf{q}_1\cdot(\mathbf{m}-\mathbf{n})$	$q_2^2+\mathbf{q}_2\cdot(\mathbf{m}-\mathbf{n})$
I.2	$\lvert\mathbf{q}-\mathbf{q}_1\rvert$	$\lvert\mathbf{q}_1-\mathbf{q}_2\rvert$	$\mathbf{q}_2$	$\lvert\mathbf{n}-\mathbf{m}-\mathbf{q}_2\rvert$	$q_1^2+\mathbf{q}_1\cdot(\mathbf{m}-\mathbf{n})$	$q_1^2-q_2^2+(\mathbf{q}_1-\mathbf{q}_2)\cdot(\mathbf{m}-\mathbf{n})$
I.3+4	$\lvert\mathbf{q}_2-\mathbf{q}_1\rvert$	$\lvert\mathbf{q}-\mathbf{q}_2\rvert$	$\mathbf{q}_1$	$\lvert\mathbf{n}-\mathbf{m}-\mathbf{q}_1\rvert$	$q_1^2+\mathbf{q}_1\cdot(\mathbf{m}-\mathbf{n})$	$q^2-q_2^2+(\mathbf{q}-\mathbf{q}_2)\cdot(\mathbf{m}-\mathbf{n})$
I.6	$\lvert\mathbf{q}-\mathbf{q}_2\rvert$	$\lvert\mathbf{q}_2-\mathbf{q}_1\rvert$	$\mathbf{q}_1$	$\lvert\mathbf{n}-\mathbf{m}-\mathbf{q}_1\rvert$	$q^2-q_1^2+(\mathbf{q}-\mathbf{q}_1)\cdot(\mathbf{m}-\mathbf{n})$	$q^2-q_2^2+(\mathbf{q}-\mathbf{q}_2)\cdot(\mathbf{m}-\mathbf{n})$
IA.1	$\lvert\mathbf{n}-\mathbf{m}-\mathbf{q}\rvert$	$\lvert\mathbf{q}_1-\mathbf{m}\rvert$	$\lvert\mathbf{q}_1-\mathbf{q}_2\rvert$	$\lvert\mathbf{n}-\mathbf{q}-\mathbf{q}_2\rvert$	$q^2+\mathbf{q}\cdot(\mathbf{q}_1-\mathbf{n})$	$q^2+\mathbf{q}\cdot(\mathbf{q}_2-\mathbf{n})$
IA.2	$\lvert\mathbf{n}-\mathbf{m}-\mathbf{q}\rvert$	$\lvert\mathbf{q}_2-\mathbf{q}_1-\mathbf{q}\rvert$	$\lvert\mathbf{n}-\mathbf{q}_1-\mathbf{q}\rvert$	$\lvert\mathbf{q}_2-\mathbf{m}-\mathbf{q}\rvert$	$2q^2+\mathbf{q}\cdot(\mathbf{m}+\mathbf{q}_1-\mathbf{n}-\mathbf{q}_2)$	$q^2+\mathbf{q}\cdot(\mathbf{m}-\mathbf{q}_2)$
IA.3	$\lvert\mathbf{n}-\mathbf{m}-\mathbf{q}\rvert$	$\lvert\mathbf{n}-\mathbf{q}_1\rvert$	$\lvert\mathbf{q}_2-\mathbf{m}\rvert$	$\lvert\mathbf{q}_2-\mathbf{q}_1+\mathbf{q}\rvert$	$q^2+\mathbf{q}\cdot(\mathbf{m}-\mathbf{q}_1)$	$q^2+\mathbf{q}\cdot(\mathbf{q}_2-\mathbf{q}_1)$

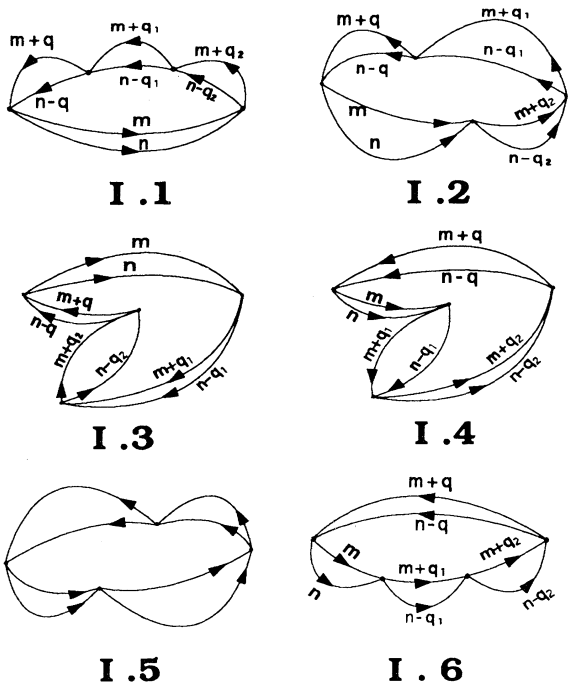

FIG. 1. Class I, fourth-order perturbation theory diagrams.

Of the problems of interest in the case of two-particle species, the dense cases such as He^3 are not yet adequately treated by this method. They have an estimated error of the order of 10%. For the more dilute cases, such as neutron matter, the error is a much more satisfactory estimated 1%. This feature has encouraged us to extend the results for four-particle species, since nuclear matter is a relatively dilute system, compared to close-packing density.

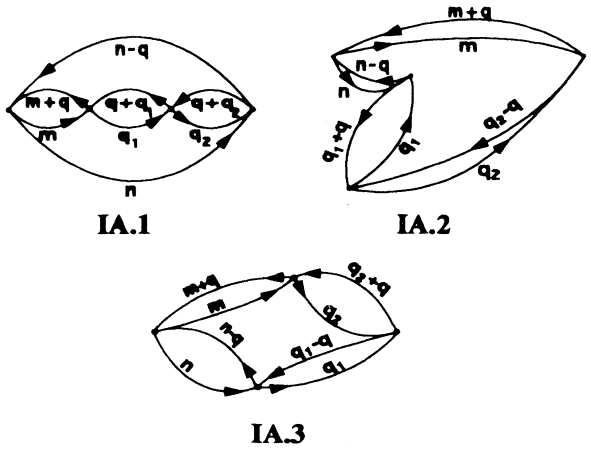

FIG. 2. Class I A, fourth-order perturbation theory diagrams.

The basic idea of quantum thermodynamic perturbation theory is similar to thermodynamic perturbation theory and seemingly goes back to Van der Waals. It was he who suggested that the description of fluids could be best started by dividing the pair interactions into a repulsive and an attractive part. The second step is to develop an accurate description of the fluid of particles with repulsive cores. The final step is to add the attraction by means of perturbation theory. This clever idea has recently been vindicated when both classical and quantum-mechanical computer simulations showed that the hard-sphere pair distribution functions are qualitatively similar [20] to those of a *liquid* whose particles interact via a Lennard-Jones potential. It has also been observed [21]

TABLE II. Arguments of the potentials and the denominators for the diagrams of classes II and II A.

Diagram	x_1	x_2	x_3	x_4	x_5	x_6	D_2	D_3
II.1	q	$\lvert q-q_1\rvert$	$\lvert n-m-q-q_1\rvert$	q_1	$\lvert n-q_2\rvert$	$\lvert q_2-q_1-m\rvert$	$q_1^2+q_1\cdot(m-n)$	$q_1^2+q_1\cdot(m-q_2)$
II.4	q	q_1	$\lvert n-m-q_1\rvert$	$\lvert q-q_1\rvert$	$\lvert n-q_2-q_1\rvert$	$\lvert q_2-q-m\rvert$	$q^2-q_1^2+(q-q_1)\cdot(m-n)$	$q^2+q\cdot(m-q_1-q_2)+q_1\cdot(q_2-m)$
II.5	q	q_1	$\lvert n-m-q_1\rvert$	$\lvert q-q_1\rvert$	$\lvert q_2-q_1-m\rvert$	$\lvert n-q-q_2\rvert$	$q_1^2+q_1\cdot(m-n)$	$q^2+q\cdot(q_2-n)+q_1^2+q_1\cdot(m-q_2-q)$
II.6	q_1	$\lvert q_1-q\rvert$	$\lvert q_2-q_1-m\rvert$	q	$\lvert n-m-q\rvert$	$\lvert n-q-q_2\rvert$	$q^2+q\cdot(q_2-n)$	$q^2+q\cdot(q_2-n)+q_1^2+q_1\cdot(m-q_2-q)$
II.7	q	$\lvert q+q_1\rvert$	$\lvert n-m-q-q_1\rvert$	q_1	$\lvert q_2-q-m\rvert$	$\lvert n-q-q_1-q_2\rvert$	$q^2+q\cdot(m-n+q_1)+q_1^2+q_1\cdot(q_2-n)$	$q_1\cdot(q_2-q-m)$
II.9	q	$\lvert q+q_1\rvert$	$\lvert n-m-q+q_1\rvert$	q_1	$\lvert n-q_2\rvert$	$\lvert q_2+q_1-m\rvert$	$q^2+q\cdot(m-n)+q_1\cdot(q_2-n)$	$q^2-q_1^2+(q+q_1)\cdot(m-n)$
II.10	q_1	$\lvert q-q_1\rvert$	$\lvert q_2-q-m\rvert$	q	$\lvert n-m-q\rvert$	$\lvert q_2+q_1-n\rvert$	$q^2+q\cdot(m-n)+q_1\cdot(q_2-m)$	$q\cdot(q_2+q_1-n)$
II.11	q	$\lvert q-q_1\rvert$	$\lvert n-m-q-q_1\rvert$	q_1	$\lvert n-q_2\rvert$	$\lvert q_2-q_1-m\rvert$	$q_1^2+q_1\cdot(m-q_2)$	$q^2+q\cdot(m-n)-q_1\cdot(q_2-n)$
IIA.1	q	$\lvert n-m-q\rvert$	q_1	$\lvert n-q-q_1-q_2\rvert$	$\lvert n-m-q-q_1\rvert$	$\lvert n-q_1-q_2\rvert$	$q_1^2+q_1\cdot(q_2-n)$	$q^2+q\cdot(q_1+m-n)+q_1^2+q_1\cdot(q_2-n)$
IIA.2	q	$\lvert n-m-q\rvert$	q_1	$\lvert n-q-q_1-q_2\rvert$	$\lvert n-m-q-q_1\rvert$	$\lvert n-q_1-q_2\rvert$	$q^2+q\cdot(m-n+q_1)$	$q^2+q\cdot(q_1+m-n)+q_1^2+q_1\cdot(q_2-n)$
IIA.3	q	$\lvert n-m-q\rvert$	q_1	$\lvert n-q_2\rvert$	$\lvert n-m-q+q_1\rvert$	$\lvert n-q-q_2\rvert$	$q^2+q\cdot(m-n)+q_1\cdot(q_2-n)$	$q_1\cdot(q_2+q-n)$
IIA.5	$\lvert q_1-q\rvert$	$\lvert q_2-m-q\rvert$	$\lvert n-m-q\rvert$	q	$\lvert n-q_2\rvert$	q_1	$q^2+q\cdot(m-n-q_1)-q_1\cdot(m-n)$	$q^2+q\cdot(m-q_1-q_2)+q_1\cdot(q_2-m)$
IIA.6	$\lvert q_1-q\rvert$	$\lvert n-q+q_1-q_2\rvert$	$\lvert n-m-q\rvert$	q	$\lvert q_2-q_1-m\rvert$	q_1	$q^2+q\cdot(m-n-q_1)-q_1\cdot(m-n)$	$(q-q_1)^2+(q-q_1)\cdot(q_2-n)$

TABLE III. Arguments of the potentials and the denominators for the diagrams of class III.

Diagram	x_2	x_3	D_3
III.1	q_1	$\lvert q_2 - q_1 - q - m \rvert$	$q^2 + q\cdot(m-n) + q_1^2 + q_1\cdot(q+m-q_2)$
III.2	$\lvert n - q_2 \rvert$	$\lvert n - q_1 \rvert$	$q^2 + q\cdot(m-n) + n^2 - n\cdot(q_1+q_2) + q_1\cdot q_2$
III.7+8	q_1	$\lvert m - q_1 - q_2 \rvert$	$q_1^2 - q_1\cdot(m-q_2)$
III.9+10	$\lvert q+m-q_1 \rvert$	$\lvert m+q-q_2 \rvert$	$(q+m)^2 - (q+m)\cdot(q_1+q_2) + q_1\cdot q_2$

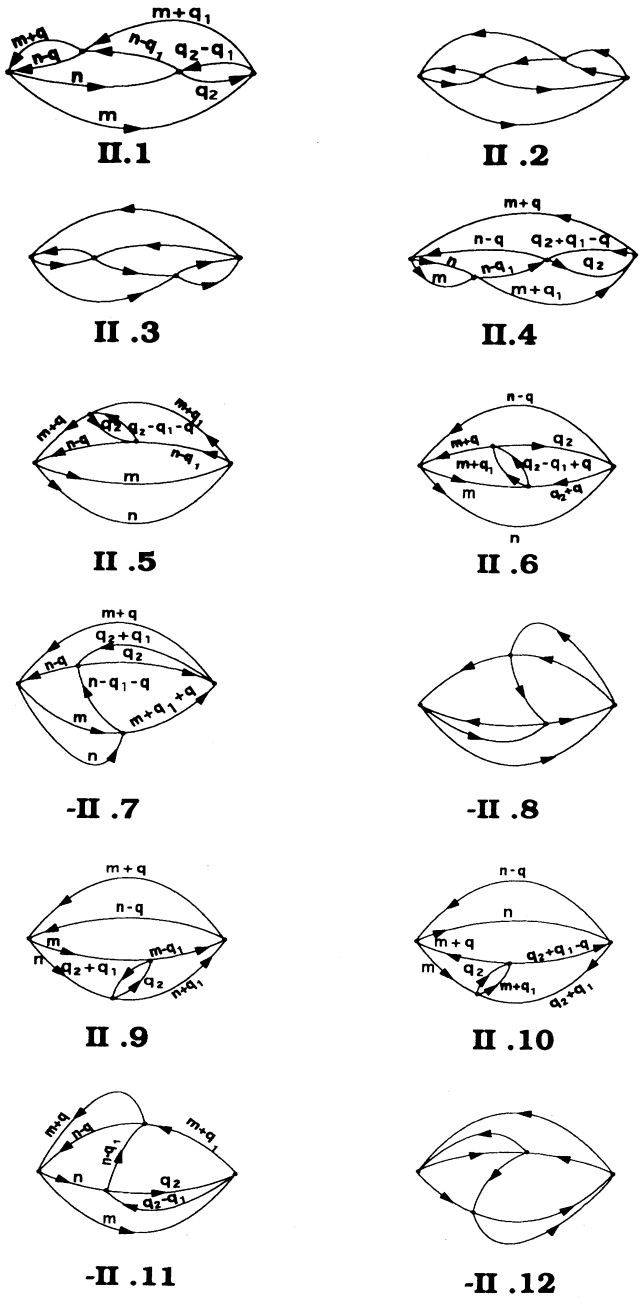

FIG. 3. Class II, fourth-order perturbation theory diagrams.

that the pair distribution of an *amorphous solid* (such as Ni-P metallic alloy glass) is remarkably similar to that [22] of a classical random close-packing arrangement. By way of contrast, the pair distribution function of the ideal gas is quite different. Our efforts in this paper are relevant to the second step described above.

The L-expansion method, which we use to estimate the ground-state energy of hard-sphere Fermi fluids, differs from the well-known K-matrix expansion [23] in the following way. In the K-matrix expansion, the Rayleigh-Schrödinger perturbation series is rearranged. Infinite sums of diagrams replace the interaction vertices, and the class of diagrams to be considered is correspondingly reduced. In the L expansion, instead, the K-matrix energy itself is expanded in powers of the interaction potential and so too is the complete ground-state energy [11]. The K-matrix energy or "ladder approximation" series is re-

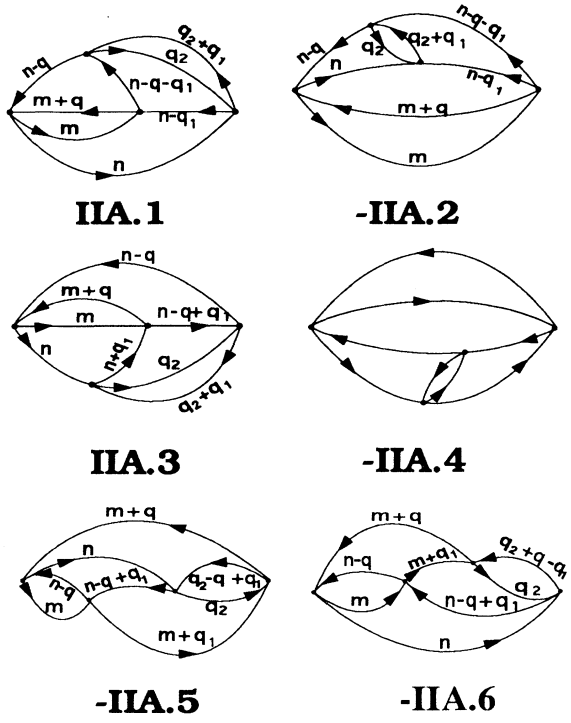

FIG. 4. Class II A, fourth-order perturbation theory diagrams.

verted to give an expansion of the interaction strength in terms of the ladder energy. This series is then substituted back into the series for the complete energy, and there then results an expansion for the complete, Fermi-fluid, ground-state energy in terms of the ladder energy. This procedure has several advantages. First of all the ladder energy remains finite in the limit of an infinite (finite-ranged) repulsive core. Second, the ladder energy can be computed [24] reasonably well by the solution of an integral equation. Third, the ladder energy is exact in the low density limit. The kinetic energy in this limit is of the order of $(k_F c)^2$, the ladder energy is of the order of $(k_F c)^3$, and the deviation of the complete energy is of the order of $(k_F c)^5$, where k_F is the Fermi momentum and c is the hard-core radius. The addition of further terms in the L expansion beyond the first reduces the order of the error in the low density limit or, expressed otherwise, increases the range of density over which this method gives good, accurate results.

In the second section, we detail the necessary fourth-order Hugenholtz diagrams. We tell how the corresponding integrals were obtained, which give the values of the diagrams, and how we coded them for a computer. We give, in tabular form, the results that we have obtained. Finally, we describe the checks that we have made to ensure their accuracy. In the course of performing these checks, we have discovered a single error in some previous work. We point out which previous results need to be replaced and, indeed, do so, except for the R-matrix computations.

In the third section we extend the L expansion and analyze some of the consequences. We find that the additional term has, in fact, improved the estimate of accuracy of this expansion, and we now feel that we have obtained good accuracy for the ground-state energy of a four-particle species, hard-sphere, Fermi fluid from low densities up through a range of densities, which includes that of nuclear matter.

II. FOURTH-ORDER HUGENHOLTZ DIAGRAMS

As in I, ν will be used to denote the number of particle species in the Fermi fluid under discussion: $\nu=4$ Fermi fluid means a Fermi fluid involving four-particle species (as in nuclear matter).

It is not difficult to generalize the expressions for the fourth-order Hugenholtz diagrams presented for the $\nu=2$ case in Sec. II of Ref. [25]. (We shall follow the notation established by those authors.) In the diagrams below "particle lines" carry leftward arrows, while "hole lines" carry rightward ones. The expressions for the fourth-order diagrams for arbitrary ν are presented below. They all involve the function

$$\phi(q)=\frac{4\pi[\sin(qk_Fc)-q(k_Fc)\cos(qk_Fc)]}{q^3}\ , \tag{2.1}$$

which is the Fourier transform of the central repulsive factor

$$\Phi(r)=\begin{cases}1, & 0\le r\le c\\ 0, & c<r\end{cases} \tag{2.2}$$

in the pair potential $V(r)$ for hard spheres, where,

$$V(r)=\left[\frac{\hbar^2}{Mc^2}\right]v\Phi(r) \quad \text{with } v\to\infty\ . \tag{2.3}$$

The diagrams belonging to class I (illustrated in Fig. 1) correspond to contributions of the form

$$\frac{-3\nu}{2^{15}\pi^{13}(k_Fc)^6}\int d\mathbf{q}\,d\mathbf{q}_1\,d\mathbf{q}_2\,d\mathbf{m}\,d\mathbf{n}\frac{\phi(q)\phi(x_2)\phi(x_3)[\phi(x_4)-(1/\nu)\phi(x_5)]}{[q^2+\mathbf{q}\cdot(\mathbf{m}-\mathbf{n})]D_2D_3}\ , \tag{2.4}$$

while class I A diagrams (shown in Fig. 2) stand for

$$\begin{aligned}\frac{-3\nu^3}{2^{14}\pi^{13}(k_Fc)^6}\int\frac{d\mathbf{q}\,d\mathbf{q}_1\,d\mathbf{q}_2\,d\mathbf{m}\,d\mathbf{n}}{[q^2+\mathbf{q}\cdot(\mathbf{m}-\mathbf{n})]D_2D_3}&\\ \times\left\{\left[\phi(q)-\frac{1}{\nu}\phi(x_2)\right]\left[\phi(q)-\frac{1}{\nu}\phi(x_3)\right]\right.&\\ \left.\times\left[\phi(q)-\frac{1}{\nu}\phi(x_4)\right]\left[\phi(q)-\frac{1}{\nu}\phi(x_5)\right]+\left[\frac{1}{\nu^2}-\frac{1}{\nu^4}\right]\phi(x_2)\phi(x_3)\phi(x_4)\phi(x_5)\right\}\ .&\end{aligned} \tag{2.5}$$

The x's and D's belonging to these two classes are listed in Table I. The integrals for all diagrams range over all the momenta allowed by the Pauli exclusion principle. Our momenta are normalized to the Fermi momentum k_F, and so hole-line momenta (such as $|\mathbf{m}|$ in all diagrams) are restricted to be less than one, while particle-line momenta (such as $|\mathbf{q}+\mathbf{m}|$ in all diagrams) are greater than 1. As in the $\nu=2$ case, diagrams I.2 and I.5 give rise to identical contributions.

Except for an occasional minus sign, the diagrams of class II (shown in Fig. 3) and class II A (shown in Fig. 4) correspond to contributions of the form

$$\frac{-3\nu^2}{2^{14}\pi^{13}(k_Fc)^6}\int\frac{d\mathbf{q}\,d\mathbf{q}_1\,d\mathbf{q}_2\,d\mathbf{m}\,d\mathbf{n}}{[q^2+\mathbf{q}\cdot(\mathbf{m}-\mathbf{n})]D_2D_3}T(x)\ , \tag{2.6}$$

where for class II

$$T(x)=\phi(x_1)\left\{\left[\phi(x_2)-\frac{1}{\nu}\phi(x_3)\right]\left[\phi(x_4)-\frac{1}{\nu}\phi(x_5)\right]\left[\phi(x_4)-\frac{1}{\nu}\phi(x_6)\right]-\left[\frac{1}{\nu}-\frac{1}{\nu^3}\right]\phi(x_3)\phi(x_5)\phi(x_6)\right\} \tag{2.7}$$

and for class II A

$$\begin{aligned}T(x)=&\phi^2(x_1)[\phi^2(x_3)+\phi(x_4)\phi(x_6)]+\phi(x_2)\phi^2(x_3)\phi(x_5)\\&-\frac{1}{\nu}\{\phi(x_3)[\phi^2(x_1)+\phi(x_2)\phi(x_5)][\phi(x_4)+\phi(x_6)]+\phi(x_1)[\phi^2(x_3)+\phi(x_4)\phi(x_6)][\phi(x_2)+\phi(x_5)]\}\\&+\frac{1}{\nu^2}\{\phi(x_1)\phi(x_3)[\phi(x_2)+\phi(x_5)][\phi(x_4)+\phi(x_6)]+\phi(x_2)\phi(x_4)\phi(x_5)\phi(x_6)\}\ .\end{aligned} \tag{2.8}$$

The x's and D's are supplied in Table II. The contribution of II.2 is identical with that of II.1, II.3 with II.4, II.7 with II.12, II.8 with II.11, and II A.4 with II A.2. It is very important to remark that equation (2.6) is off by the factor (-1) for diagrams II.7, II.8, II.11, II.12, II A.2, II A.4, II A.5, and II A.6.

For the diagrams of class III (see Fig. 5) one needs to write

$$\frac{-3\nu^2}{2^{14}\pi^{13}(k_Fc)^6}\int\frac{d\mathbf{q}\,d\mathbf{q}_1\,d\mathbf{q}_2\,d\mathbf{m}\,d\mathbf{n}}{[q^2+\mathbf{q}\cdot(\mathbf{m}-\mathbf{n})]^2D_3}\left\{\left[\phi(q)-\frac{1}{\nu}\phi(|\mathbf{n}-\mathbf{m}-\mathbf{q}|)\right]\phi(x_2)\left[\phi(x_2)-\frac{1}{\nu}\phi(x_3)\right]\right\} \tag{2.9}$$

with the appropriate x's and D_3's given in Table III. The above expression needs to be corrected by a factor of (-1) for diagrams III.7, III.8, III.9, and III.10. Note that diagrams III.3, III.4, III.5, III.6, III.11, and III.12 give zero contributions because they each involve a particle and hole line with the same momentum.

It seems least inconvenient to list the distinct contributions from class IV (Fig. 6) diagrams individually:

(IV.1)

$$\begin{aligned}&\frac{-3\nu}{2^{15}\pi^{13}(k_Fc)^6}\int\frac{d\mathbf{q}\,d\mathbf{q}_1\,d\mathbf{q}_2\,d\mathbf{m}\,d\mathbf{n}}{[q^2+\mathbf{q}\cdot(\mathbf{m}-\mathbf{n})]^3}\phi(q)\left[\phi(q)-\frac{1}{\nu}\phi(|\mathbf{n}-\mathbf{m}-\mathbf{q}|)\right]\\&\times[\phi(|\mathbf{q}+\mathbf{q}_1+\mathbf{m}|)-\phi(|\mathbf{q}_1+\mathbf{m}|)+\phi(|\mathbf{q}_1+\mathbf{n}-\mathbf{q}|)-\phi(|\mathbf{q}_1+\mathbf{n}|)]\\&\times[\phi(|\mathbf{q}+\mathbf{q}_2+\mathbf{m}|)-\phi(|\mathbf{q}_2+\mathbf{m}|)+\phi(|\mathbf{q}_2+\mathbf{n}-\mathbf{q}|)-\phi(|\mathbf{q}_2+\mathbf{n}|)]\ ,\end{aligned} \tag{2.10}$$

(IV.2, IV.3)

$$\begin{aligned}&\frac{+3\nu}{2^{14}\pi^{13}(k_Fc)^6}\int\frac{d\mathbf{q}\,d\mathbf{q}_1\,d\mathbf{q}_2\,d\mathbf{m}\,d\mathbf{n}}{[q^2+\mathbf{q}\cdot(\mathbf{m}-\mathbf{n})]^2[q_1^2+\mathbf{q}_1\cdot(\mathbf{m}-\mathbf{n})]}\phi(q)\phi(|\mathbf{q}-\mathbf{q}_1|)\\&\times\left[\phi(q_1)-\frac{1}{\nu}\phi(|\mathbf{q}_1+\mathbf{m}-\mathbf{n}|)\right][\phi(|\mathbf{q}+\mathbf{q}_2+\mathbf{m}|)-\phi(|\mathbf{q}_2+\mathbf{m}|)]\ ,\end{aligned} \tag{2.11}$$

(IV.4, IV.5)

$$\begin{aligned}&\frac{+3\nu^2}{2^{14}\pi^{13}(k_Fc)^6}\int\frac{d\mathbf{q}\,d\mathbf{q}_1\,d\mathbf{q}_2\,d\mathbf{m}\,d\mathbf{n}}{[q^2+\mathbf{q}\cdot(\mathbf{m}-\mathbf{n})]^2[q^2+\mathbf{q}\cdot(\mathbf{m}-\mathbf{q}_1)]}\\&\times\left\{\left[\phi(q)-\frac{1}{\nu}\phi(|\mathbf{q}+\mathbf{m}-\mathbf{n}|)\right]\left[\phi(q)-\frac{1}{\nu}\phi(|\mathbf{q}_1-\mathbf{n}|)\right]\right.\\&\times\left[\phi(q)-\frac{1}{\nu}\phi(|\mathbf{q}+\mathbf{m}-\mathbf{q}_1|)\right]-\left.\left[\frac{1}{\nu}-\frac{1}{\nu^3}\right]\phi(|\mathbf{q}+\mathbf{m}-\mathbf{n}|)\phi(|\mathbf{q}_1-\mathbf{n}|)\phi(|\mathbf{q}+\mathbf{m}-\mathbf{q}_1|)\right\}\\&\times[\phi(|\mathbf{q}+\mathbf{m}+\mathbf{q}_2|)-\phi(|\mathbf{m}+\mathbf{q}_2|)+\phi(|\mathbf{n}+\mathbf{q}_2-\mathbf{q}|)-\phi(|\mathbf{n}+\mathbf{q}_2|)]\ ,\end{aligned} \tag{2.12}$$

(IV.6, IV.7)

$$\begin{aligned}&\frac{+3\nu}{2^{14}\pi^{13}(k_Fc)^6}\int\frac{d\mathbf{q}\,d\mathbf{q}_1\,d\mathbf{q}_2\,d\mathbf{m}\,d\mathbf{n}\phi(q)\phi(|\mathbf{q}-\mathbf{q}_1|)}{[q^2+\mathbf{q}\cdot(\mathbf{m}-\mathbf{n})]^2[q^2-q_1^2+(\mathbf{q}-\mathbf{q}_1)\cdot(\mathbf{m}-\mathbf{n})]}\\&\times\left[\phi(q_1)-\frac{1}{\nu}\phi(|\mathbf{q}_1+\mathbf{m}-\mathbf{n}|)\right][\phi(|\mathbf{q}+\mathbf{m}+\mathbf{q}_2|)-\phi(|\mathbf{m}+\mathbf{q}_2|)]\ .\end{aligned} \tag{2.13}$$

TABLE IV. Values for fourth-order Hugenholtz diagrams when $\nu=4$.

	$k_Fc=.250$		$k_Fc=.500$		$k_Fc=.750$		$k_Fc=1.00$	
Diagram	Value	Deviation	Value	Deviation	Value	Deviation	Value	Deviation
I.1	-7.530×10^{-5}	6.01×10^{-7}	-3.859×10^{-4}	1.86×10^{-6}	-7.730×10^{-4}	3.35×10^{-6}	-1.002×10^{-3}	4.89×10^{-6}
I.2	-1.845×10^{-7}	1.45×10^{-9}	-4.176×10^{-6}	1.71×10^{-8}	-2.079×10^{-5}	6.67×10^{-8}	-5.288×10^{-5}	1.54×10^{-7}
I.3+4	-1.855×10^{-7}	1.66×10^{-9}	-4.192×10^{-6}	1.65×10^{-8}	-2.079×10^{-5}	6.63×10^{-8}	-5.250×10^{-5}	1.65×10^{-7}
I.5	-1.845×10^{-7}	1.45×10^{-9}	-4.176×10^{-6}	1.71×10^{-8}	-2.079×10^{-5}	6.67×10^{-8}	-5.288×10^{-5}	1.54×10^{-7}
I.6	-2.980×10^{-9}	1.85×10^{-11}	-1.682×10^{-7}	9.82×10^{-10}	-1.564×10^{-6}	8.91×10^{-9}	-6.672×10^{-6}	3.81×10^{-8}
IA.1	-1.209×10^{-7}	7.89×10^{-10}	-6.246×10^{-6}	3.89×10^{-8}	-5.389×10^{-5}	3.45×10^{-7}	-2.120×10^{-4}	1.33×10^{-6}
IA.2	-5.615×10^{-8}	1.17×10^{-9}	-2.981×10^{-6}	4.51×10^{-8}	-2.505×10^{-5}	2.25×10^{-7}	-1.022×10^{-4}	7.63×10^{-7}
IA.3	-1.108×10^{-7}	4.11×10^{-10}	-5.842×10^{-6}	2.12×10^{-8}	-4.907×10^{-5}	1.73×10^{-7}	-1.960×10^{-4}	7.75×10^{-7}
II.1	-7.825×10^{-7}	1.01×10^{-8}	-1.446×10^{-5}	9.49×10^{-8}	-6.148×10^{-5}	3.99×10^{-7}	-1.428×10^{-4}	1.11×10^{-6}
II.2	-7.825×10^{-7}	1.01×10^{-8}	-1.446×10^{-5}	9.49×10^{-8}	-6.148×10^{-5}	3.99×10^{-7}	-1.428×10^{-4}	1.11×10^{-6}
II.3	-7.009×10^{-9}	2.48×10^{-11}	-3.681×10^{-7}	1.25×10^{-9}	-3.088×10^{-6}	1.22×10^{-8}	-1.223×10^{-5}	6.33×10^{-8}
II.4	-7.009×10^{-9}	2.48×10^{-11}	-3.681×10^{-7}	1.25×10^{-9}	-3.088×10^{-6}	1.22×10^{-8}	-1.223×10^{-5}	6.33×10^{-8}
II.5	-1.684×10^{-7}	2.28×10^{-9}	-4.302×10^{-6}	4.46×10^{-8}	-2.234×10^{-5}	2.17×10^{-7}	-6.350×10^{-5}	5.70×10^{-7}
II.6	-6.604×10^{-7}	6.71×10^{-9}	-1.221×10^{-5}	6.59×10^{-8}	-5.346×10^{-5}	5.07×10^{-7}	-1.254×10^{-4}	8.95×10^{-7}
II.7	$+7.975\times10^{-9}$	1.09×10^{-10}	$+4.275\times10^{-7}$	4.35×10^{-9}	$+3.721\times10^{-6}$	2.95×10^{-8}	$+1.547\times10^{-5}$	1.29×10^{-7}
II.8	$+1.373\times10^{-8}$	1.51×10^{-10}	$+6.811\times10^{-7}$	5.37×10^{-9}	$+5.690\times10^{-6}$	4.39×10^{-8}	$+2.297\times10^{-5}$	1.94×10^{-7}
II.9	-4.387×10^{-9}	2.79×10^{-11}	-2.489×10^{-7}	1.50×10^{-9}	-2.434×10^{-6}	1.44×10^{-8}	-1.085×10^{-5}	6.39×10^{-8}
II.10	-1.512×10^{-9}	1.22×10^{-11}	-8.177×10^{-8}	7.07×10^{-10}	-7.493×10^{-7}	7.28×10^{-9}	-3.201×10^{-6}	4.21×10^{-8}
II.11	$+1.373\times10^{-8}$	1.51×10^{-10}	$+6.811\times10^{-7}$	5.37×10^{-9}	$+5.690\times10^{-6}$	4.39×10^{-8}	$+2.297\times10^{-5}$	1.94×10^{-7}
II.12	$+7.975\times10^{-9}$	1.09×10^{-10}	$+4.275\times10^{-7}$	4.35×10^{-9}	$+3.721\times10^{-6}$	2.95×10^{-8}	$+1.547\times10^{-5}$	1.29×10^{-7}
IIA. 1	-1.706×10^{-6}	9.74×10^{-9}	-4.884×10^{-5}	9.49×10^{-8}	-2.672×10^{-4}	4.38×10^{-7}	-7.283×10^{-4}	1.20×10^{-6}
IIA.2	$+6.139\times10^{-8}$	1.62×10^{-10}	$+3.314\times10^{-6}$	8.56×10^{-9}	$+2.927\times10^{-5}$	7.34×10^{-8}	$+1.185\times10^{-4}$	3.25×10^{-7}
IIA.3	-1.403×10^{-8}	6.98×10^{-11}	-8.221×10^{-7}	5.52×10^{-9}	-8.189×10^{-6}	5.50×10^{-8}	-3.749×10^{-5}	2.49×10^{-7}
IIA.4	$+6.139\times10^{-8}$	1.62×10^{-10}	$+3.314\times10^{-6}$	8.56×10^{-9}	$+2.927\times10^{-5}$	7.34×10^{-8}	$+1.185\times10^{-4}$	3.25×10^{-7}
IIA.5	$+1.034\times10^{-7}$	1.85×10^{-10}	$+5.347\times10^{-6}$	7.75×10^{-9}	$+4.473\times10^{-5}$	6.13×10^{-8}	$+1.695\times10^{-4}$	2.70×10^{-7}
IIA.6	$+9.666\times10^{-8}$	3.11×10^{-10}	$+5.050\times10^{-6}$	1.72×10^{-8}	$+4.209\times10^{-5}$	1.33×10^{-7}	$+1.586\times10^{-4}$	4.96×10^{-7}
III.1	-2.598×10^{-6}	2.32×10^{-8}	-5.400×10^{-5}	3.47×10^{-7}	-2.628×10^{-4}	1.10×10^{-6}	-6.814×10^{-4}	2.35×10^{-6}
III.2	-4.127×10^{-8}	1.48×10^{-10}	-2.313×10^{-6}	1.35×10^{-8}	-2.074×10^{-5}	7.05×10^{-8}	-8.730×10^{-5}	4.98×10^{-7}
III.7+8	$+3.272\times10^{-6}$	2.75×10^{-8}	$+7.357\times10^{-5}$	3.08×10^{-7}	$+3.688\times10^{-4}$	1.50×10^{-6}	$+9.755\times10^{-4}$	3.67×10^{-6}
III.9+10	$+6.091\times10^{-8}$	2.32×10^{-10}	$+3.258\times10^{-6}$	1.72×10^{-8}	$+2.751\times10^{-5}$	1.54×10^{-7}	$+1.802\times10^{-4}$	7.76×10^{-7}
IV.1	-2.099×10^{-11}	3.40×10^{-12}	-1.030×10^{-8}	2.30×10^{-10}	-2.825×10^{-7}	2.13×10^{-9}	-2.602×10^{-6}	1.08×10^{-8}
IV.2	-4.054×10^{-8}	1.41×10^{-9}	-1.965×10^{-6}	2.00×10^{-8}	-1.448×10^{-5}	1.31×10^{-7}	-4.911×10^{-5}	3.42×10^{-7}
IV.3	-4.054×10^{-8}	1.41×10^{-9}	-1.965×10^{-6}	2.00×10^{-8}	-1.448×10^{-5}	1.31×10^{-7}	-4.911×10^{-5}	3.42×10^{-7}
IV.4	-4.697×10^{-10}	5.85×10^{-12}	-8.028×10^{-8}	5.98×10^{-10}	-1.321×10^{-6}	8.37×10^{-9}	-8.676×10^{-6}	5.74×10^{-8}
IV.5	-4.697×10^{-10}	5.85×10^{-12}	-8.028×10^{-8}	5.98×10^{-10}	-1.321×10^{-6}	8.37×10^{-9}	-8.676×10^{-6}	5.74×10^{-8}
IV.6	$+1.144\times10^{-10}$	1.80×10^{-12}	$+2.219\times10^{-8}$	2.09×10^{-10}	$+4.166\times10^{-7}$	3.50×10^{-9}	$+2.753\times10^{-6}$	2.91×10^{-8}
IV.7	$+1.144\times10^{-10}$	1.80×10^{-12}	$+2.219\times10^{-8}$	2.09×10^{-10}	$+4.166\times10^{-7}$	3.50×10^{-9}	$+2.753\times10^{-6}$	2.91×10^{-8}

TABLE IV. (*Continued*).

	k_Fc=1.25		k_Fc=1.50		k_Fc=2.00		k_Fc=3.00	
Diagram	Value	Deviation	Value	Deviation	Value	Deviation	Value	Deviation
I.1	-9.864×10^{-4}	4.84×10^{-6}	-8.517×10^{-4}	6.74×10^{-6}	-5.273×10^{-4}	8.16×10^{-6}	-2.907×10^{-4}	1.79×10^{-5}
I.2	-9.238×10^{-5}	3.43×10^{-7}	-1.225×10^{-4}	5.75×10^{-7}	-1.247×10^{-4}	1.11×10^{-6}	-7.991×10^{-5}	2.74×10^{-6}
I.3+4	-8.944×10^{-5}	3.18×10^{-7}	-1.163×10^{-4}	5.43×10^{-7}	-1.138×10^{-4}	1.07×10^{-6}	-6.659×10^{-5}	2.16×10^{-6}
I.5	-9.238×10^{-5}	3.43×10^{-7}	-1.225×10^{-4}	5.75×10^{-7}	-1.247×10^{-4}	1.11×10^{-6}	-7.991×10^{-5}	2.74×10^{-6}
I.6	-1.802×10^{-5}	1.06×10^{-7}	-3.567×10^{-5}	2.24×10^{-7}	-7.367×10^{-5}	6.33×10^{-7}	-8.296×10^{-5}	2.60×10^{-6}
IA.1	-5.535×10^{-4}	3.45×10^{-6}	-1.159×10^{-3}	9.88×10^{-6}	-3.304×10^{-3}	3.53×10^{-5}	-1.361×10^{-2}	3.04×10^{-4}
IA.2	-2.794×10^{-4}	1.85×10^{-6}	-6.163×10^{-4}	4.41×10^{-6}	-1.992×10^{-3}	2.01×10^{-5}	-8.456×10^{-3}	1.40×10^{-4}
IA.3	-5.187×10^{-4}	2.20×10^{-6}	-1.076×10^{-3}	5.82×10^{-6}	-3.165×10^{-3}	2.69×10^{-5}	-1.301×10^{-2}	2.27×10^{-4}
II.1	-2.537×10^{-4}	2.58×10^{-6}	-4.120×10^{-4}	5.04×10^{-6}	-9.104×10^{-4}	1.44×10^{-5}	-1.970×10^{-3}	8.84×10^{-5}
II.2	-2.537×10^{-4}	2.58×10^{-6}	-4.120×10^{-4}	5.04×10^{-6}	-9.104×10^{-4}	1.44×10^{-5}	-1.970×10^{-3}	8.84×10^{-5}
II.3	-3.177×10^{-5}	2.56×10^{-7}	-6.495×10^{-5}	5.97×10^{-7}	-2.020×10^{-4}	2.69×10^{-6}	-7.244×10^{-4}	1.65×10^{-5}
II.4	-3.177×10^{-5}	2.56×10^{-7}	-6.495×10^{-5}	5.97×10^{-7}	-2.020×10^{-4}	2.69×10^{-6}	-7.244×10^{-4}	1.65×10^{-5}
II.5	-1.396×10^{-4}	1.39×10^{-6}	-2.573×10^{-4}	1.92×10^{-6}	-6.193×10^{-4}	5.11×10^{-6}	-1.169×10^{-3}	1.75×10^{-5}
II.6	-2.250×10^{-4}	2.02×10^{-6}	-3.510×10^{-4}	3.93×10^{-6}	-6.509×10^{-4}	8.10×10^{-6}	-1.286×10^{-3}	5.62×10^{-5}
II.7	$+4.277\times10^{-5}$	3.78×10^{-7}	$+9.201\times10^{-5}$	8.90×10^{-7}	$+2.724\times10^{-4}$	3.35×10^{-6}	$+7.572\times10^{-4}$	2.49×10^{-5}
II.8	$+6.099\times10^{-5}$	6.28×10^{-7}	$+1.296\times10^{-4}$	1.69×10^{-6}	$+3.214\times10^{-4}$	6.24×10^{-6}	$+7.585\times10^{-4}$	3.14×10^{-5}
II.9	-3.201×10^{-5}	2.62×10^{-7}	-7.224×10^{-5}	1.28×10^{-6}	-2.132×10^{-4}	3.03×10^{-6}	-6.454×10^{-4}	1.77×10^{-5}
II.10	-8.470×10^{-6}	1.41×10^{-7}	-1.955×10^{-5}	4.05×10^{-7}	-6.928×10^{-5}	2.32×10^{-6}	-2.794×10^{-4}	1.08×10^{-5}
II.11	$+6.099\times10^{-5}$	6.28×10^{-7}	$+1.296\times10^{-4}$	1.69×10^{-6}	$+3.214\times10^{-4}$	6.24×10^{-6}	$+7.585\times10^{-4}$	3.14×10^{-5}
II.12	$+4.277\times10^{-5}$	3.78×10^{-7}	$+9.201\times10^{-5}$	8.90×10^{-7}	$+2.724\times10^{-4}$	3.35×10^{-6}	$+7.572\times10^{-4}$	2.49×10^{-5}
IIA.1	-1.367×10^{-3}	2.95×10^{-6}	-2.061×10^{-3}	5.23×10^{-6}	-3.350×10^{-3}	1.35×10^{-5}	-5.290×10^{-3}	7.03×10^{-5}
IIA.2	$+3.079\times10^{-4}$	8.84×10^{-7}	$+5.956\times10^{-4}$	1.83×10^{-6}	$+1.372\times10^{-3}$	6.19×10^{-6}	$+3.182\times10^{-3}$	4.72×10^{-5}
IIA.3	-1.096×10^{-4}	7.59×10^{-7}	-2.481×10^{-4}	1.86×10^{-6}	-6.984×10^{-4}	5.78×10^{-6}	-2.009×10^{-3}	3.53×10^{-5}
IIA.4	$+3.079\times10^{-4}$	8.84×10^{-7}	$+5.956\times10^{-4}$	1.83×10^{-6}	$+1.372\times10^{-3}$	6.19×10^{-6}	$+3.182\times10^{-3}$	4.72×10^{-5}
IIA.5	$+4.104\times10^{-4}$	7.12×10^{-7}	$+7.460\times10^{-4}$	1.37×10^{-6}	$+1.540\times10^{-3}$	4.89×10^{-6}	$+3.204\times10^{-3}$	2.63×10^{-5}
IIA.6	$+3.845\times10^{-4}$	1.28×10^{-6}	$+7.066\times10^{-4}$	2.58×10^{-6}	$+1.464\times10^{-3}$	6.92×10^{-6}	$+3.066\times10^{-3}$	4.09×10^{-5}
III.1	-1.272×10^{-3}	5.26×10^{-6}	-1.944×10^{-3}	7.65×10^{-6}	-3.288×10^{-3}	2.04×10^{-5}	-5.735×10^{-3}	9.59×10^{-5}
III.2	-2.345×10^{-4}	7.30×10^{-7}	-4.765×10^{-4}	2.34×10^{-6}	-1.172×10^{-3}	8.72×10^{-6}	-2.846×10^{-3}	4.03×10^{-5}
III.7+8	$+1.796\times10^{-3}$	6.54×10^{-6}	$+2.740\times10^{-3}$	1.57×10^{-5}	$+4.425\times10^{-3}$	3.47×10^{-5}	$+6.868\times10^{-3}$	1.02×10^{-5}
III.9+10	$+2.694\times10^{-4}$	2.13×10^{-6}	$+5.133\times10^{-4}$	4.07×10^{-6}	$+1.141\times10^{-3}$	5.53×10^{-6}	$+2.708\times10^{-3}$	5.09×10^{-5}
IV.1	-1.291×10^{-5}	3.91×10^{-8}	-4.242×10^{-5}	1.77×10^{-7}	-2.082×10^{-4}	7.13×10^{-7}	-8.110×10^{-4}	6.26×10^{-6}
IV.2	-1.112×10^{-4}	8.47×10^{-7}	-1.816×10^{-4}	1.65×10^{-6}	-3.097×10^{-4}	3.78×10^{-6}	-4.238×10^{-4}	9.30×10^{-6}
IV.3	-1.112×10^{-4}	8.47×10^{-7}	-1.816×10^{-4}	1.65×10^{-6}	-3.097×10^{-4}	3.78×10^{-6}	-4.238×10^{-4}	9.30×10^{-6}
IV.4	-3.574×10^{-5}	2.54×10^{-7}	-1.125×10^{-4}	8.42×10^{-7}	-6.187×10^{-4}	3.85×10^{-6}	-3.400×10^{-3}	5.69×10^{-5}
IV.5	-3.574×10^{-5}	2.54×10^{-7}	-1.125×10^{-4}	8.42×10^{-7}	-6.187×10^{-4}	3.85×10^{-6}	-3.400×10^{-3}	5.69×10^{-5}
IV.6	$+1.063\times10^{-5}$	1.05×10^{-7}	$+2.807\times10^{-5}$	3.28×10^{-7}	$+8.547\times10^{-5}$	1.06×10^{-6}	$+1.916\times10^{-4}$	9.59×10^{-6}
IV.7	$+1.063\times10^{-5}$	1.05×10^{-7}	$+2.807\times10^{-5}$	3.28×10^{-7}	$+8.547\times10^{-5}$	1.06×10^{-6}	$+1.916\times10^{-4}$	9.59×10^{-6}

TABLE V. Corrected values for diagrams II A.5 and I.3+4, as well as for Σ4, Δ4, p_4, and $Q(L_H)$ when $\nu=2$.

	k_{FC}=.250		k_{FC}=.500		k_{FC}=.750		k_{FC}=1.00	
Diagram	Value	Deviation	Value	Deviation	Value	Deviation	Value	Deviation
IIA.5	4.79×10^{-9}	1.5×10^{-11}	2.34×10^{-7}	6.9×10^{-10}	1.81×10^{-6}	5.7×10^{-9}	6.63×10^{-6}	2.9×10^{-8}
I.3+4	-6.30×10^{-8}	3.7×10^{-10}	-1.41×10^{-6}	4.6×10^{-9}	-6.89×10^{-6}	1.8×10^{-8}	-1.75×10^{-5}	4.9×10^{-8}
Σ4	-2.438×10^{-5}	1.9×10^{-7}	-1.152×10^{-4}	5.5×10^{-7}	-2.003×10^{-4}	1.4×10^{-6}	-2.285×10^{-4}	2.9×10^{-6}
Δ4	6.75×10^{-7}	7.0×10^{-9}	1.356×10^{-5}	3.3×10^{-7}	5.68×10^{-5}	8.7×10^{-7}	1.089×10^{-4}	2.0×10^{-6}
p_4	-7.56×10^{4}	1.1×10^{5}	1.00×10^{3}	8.5×10^{2}	66.0	16	4.91	.97
$Q(L_H)$	2.795	3×10^{-3}	2.49	2×10^{-2}	2.20	8×10^{-2}	1.93	0.2

	k_{FC}=1.25		k_{FC}=1.50		k_{FC}=2.00		k_{FC}=3.00	
Diagram	Value	Deviation	Value	Deviation	Value	Deviation	Value	Deviation
IIA.5	1.67×10^{-5}	4.7×10^{-8}	3.60×10^{-5}	2.4×10^{-7}	1.35×10^{-4}	1.1×10^{-6}	6.22×10^{-4}	1.1×10^{-5}
I.3+4	-2.99×10^{-5}	6.4×10^{-8}	-3.91×10^{-5}	1.1×10^{-7}	-4.00×10^{-5}	2.8×10^{-7}	-3.32×10^{-5}	8.0×10^{-7}
Σ4	-2.461×10^{-4}	2.13×10^{-6}	-3.26×10^{-4}	8.2×10^{-6}	-1.094×10^{-3}	2.8×10^{-5}	-5.62×10^{-3}	2.6×10^{-4}
Δ4	$+9.43\times10^{-5}$	1.54×10^{-6}	-2.50×10^{-5}	6.7×10^{-6}	-8.69×10^{-4}	2.6×10^{-5}	-5.51×10^{-3}	2.6×10^{-4}
p_4	1.89×10^{-2}	9×10^{-2}	-6.16×10^{-2}	1.6×10^{-2}	-2.31×10^{-2}	1.2×10^{-3}	-7.30×10^{-4}	4.2×10^{-5}
$Q(L_H)$	1.73	0.1	1.7	0.6	----------	--------	---------	--------

TABLE VI. Summary of new results for $\nu=4$ case.

	k_Fc=.250		k_Fc=.500		k_Fc=.750		k_Fc=1.00	
Diagram	Value	Deviation	Value	Deviation	Value	Deviation	Value	Deviation
$\Sigma 4$	-7.930×10^{-5}	6.02×10^{-7}	-4.741×10^{-4}	1.93×10^{-6}	-1.208×10^{-3}	3.98×10^{-6}	-2.039×10^{-3}	7.26×10^{-6}
$\Delta 4$	-4.001×10^{-6}	4.07×10^{-8}	-8.82×10^{-5}	5.01×10^{-7}	-4.350×10^{-4}	2.14×10^{-6}	-1.037×10^{-3}	5.37×10^{-6}
p_4	-1.32×10^{5}	6.3×10^{3}	-854	18	-35.0	.55	-2.21	4.2×10^{-2}
q_0	1.61901		1.43529		1.25353		1.08507	
L_H	5.96001×10^{-3}		6.06778×10^{-2}		0.26848		0.84934	
$Q(L_H)$	1.611	1.0×10^{-2}	1.41	5×10^{-2}	1.20	0.13	.98	0.26

	k_Fc=1.25		k_Fc=1.50		k_Fc=2.00		k_Fc=3.00	
Diagram	Value	Deviation	Value	Deviation	Value	Deviation	Value	Deviation
$\Sigma 4$	-3.191×10^{-3}	1.25×10^{-5}	-4.718×10^{-3}	2.56×10^{-5}	-1.111×10^{-2}	7.24×10^{-5}	-4.316×10^{-2}	4.69×10^{-4}
$\Delta 4$	-2.205×10^{-3}	1.15×10^{-5}	-3.866×10^{-3}	2.47×10^{-5}	-1.058×10^{-2}	7.19×10^{-5}	-4.287×10^{-2}	4.69×10^{-4}
p_4	-.388	9.0×10^{-3}	-8.41×10^{-2}	1.2×10^{-3}	-8.72×10^{-3}	9.0×10^{-5}	-2.63×10^{-4}	3.2×10^{-6}
q_0	0.93495		0.80426		0.59593		0.33896	
L_H	2.23435		5.21771		22.5266		234.997	
$Q(L_H)$	0.8	0.6	0.5	1.4				

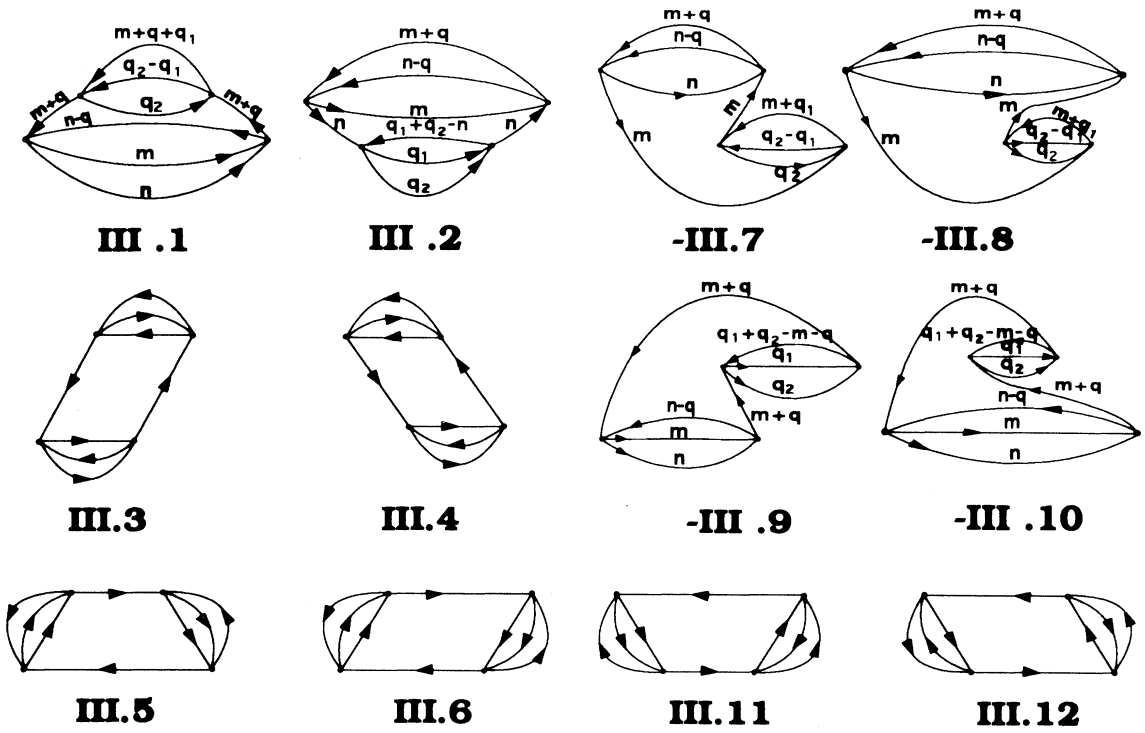

FIG. 5. Class III, fourth-order perturbation theory diagrams.

All of the preceding integrals were evaluated using Monte Carlo methods. The uncertainties in the values of the integral were successfully limited through a judicious choice of the momenta for which their integrands were sampled.

(i) The cube of the magnitude of hole-line momenta used here was uniformly distributed between 0 and 1.

(ii) The particle-line momentum magnitudes were chosen through the rule r^{-E}, where the r's were random numbers uniformly distributed between 0 and 1, and E was set so that the integrand approached a finite value as $r \rightarrow 0$.

(iii) The azimuthal angles and the cosines of polar angles associated with the momenta were assumed uniformly distributed between 0 and 2π and between -1 and $+1$, respectively.

The number of samplings ranged from 10^6 to 4×10^6 for the different diagrams. The calculations of the different diagrams converged differently, making it necessary to use different numbers of samplings. All the fourth-order Hugenholtz diagrams were evaluated for $\nu=4$ at eight different densities ($k_F c$), and the results are presented in Table IV.

Before embarking on these computations, as a check on our work, the above expressions were evaluated for $\nu=2$ and $k_F c = 1.50$ for each of the diagrams, and the resulting numbers were compared with Table III of Ref. [26]. Through this check an error was discovered in connection with diagram II A.5 as described in Ref. [27]. In Table III of Ref. [27] an appropriate set of permutations for the listed momentum transfers is (13)(12)(23) instead of the set (13)(12)(13) given there. It was also found that the values for I.3+4 in Ref. [26] are incorrect for some densities even though there is no error in the expression (25) on which the original calculations were based. Presumably the $(2-3)\times10^5$ Monte Carlo repetitions used for the original evaluation were inadequate. The corrected values for II A.5 and I.3+4 ($\nu=2$) are presented in Table V.

These changes necessitate other corrections also in previous work. In Table III of paper I both $\Sigma 4$, the sum of the contributions from all fourth-order diagrams, and $\Delta 4$, which is $\Sigma 4$ less the contribution from diagram I.1, must be corrected by referring to our Table V. Of course, the errors just mentioned infect the p_4 coefficients of the L expansion (Table V of paper I) as well as the results for $Q(L_H)$ (Table VII of paper I) for the $\nu=2$ Fermi fluid. Corrections to these results also appear in Table V. These corrections also take into account the correction to the erroneously listed value of q_0 for $k_F c = 1.25$. The correct value is 1.502 16. Relative to the quoted errors, the changes in $Q(L_H)$ (3.3) are not large and do not change the conclusions of paper I. Note is made that the quoted error in $Q(L_H)$ for $k_F c = 1.25$ may be unrealistically small, as p_4 is changing sign in that vicinity.

III. EXTENSION OF THE ANALYSIS FOR $\nu=4$ HARD-SPHERE FERMI FLUIDS

In paper I the L expansion for the ground-state energy of a Fermi fluid is given as [Eq. (5.1)]

$$\frac{\Delta E M c^2}{N\hbar^2} = L + p_3 L^3 + p_4 L^4 + \cdots , \tag{3.1}$$

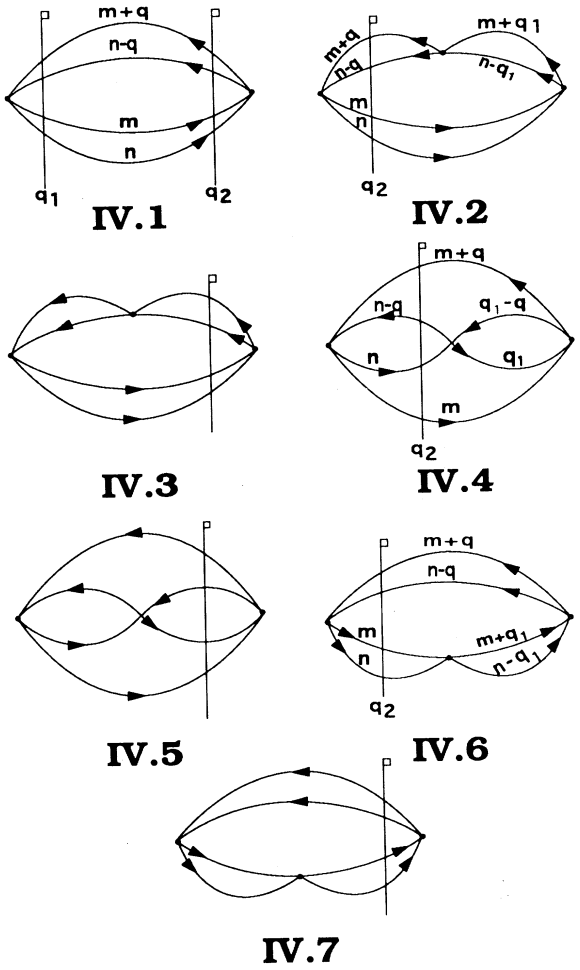

FIG. 6. Class IV, fourth-order perturbation theory diagrams.

where

$$p_3=\frac{\Delta 3}{B_1^3} \quad \text{and} \quad p_4=\frac{\Delta 4}{B_1^4}-3\frac{\Delta 3 B_2}{B_1^5} \tag{3.2}$$

with the Δi representing the sum of all ith-order Hugenholtz diagrams less the ith-order ladder diagram, and with B_1 and B_2 representing the only first- and second-order diagrams. The results of Sec. II make possible the tabulation of the p_4's for the $\nu=4$ Fermi fluid, and these are presented in Table VI. With these p_4's in combination with the p_3's of paper I, it is possible to calculate the energy of this Fermi fluid more accurately.

We have summed the available terms in the L expansion using the method of Padé approximants and estimated the errors, which we consider to be a combination of the statistical errors of Table IV and apparent errors of approximation. These latter errors are estimated by the method of Hunter and Baker [28]. Following paper I, we have studied the behavior of

$$Q(L)=\left[\frac{LN(k_F c)^3\hbar^2}{L_H \Delta E M c^2}\right]^{1/2}$$
$$=q_0\left\{1-\frac{p_3}{2}L^2-\frac{p_4}{2}L^3+O(L^4)\right\}, \tag{3.3}$$

which, as pointed out in paper I, should approach zero linearly as a function of k_F near some quantum, random, close-packing density [11]. L_H is the value of L corresponding to a hard-core potential of radius c. Our results for $Q(L_H)$ are given in Table VI. The addition of the term p_4 has not only given us more information about the values, but has allowed us to give more realistic estimates of the errors than was possible in paper I. Our current results fall roughly midway between the two alternate data summaries (based on the low-density expansion) given in paper I. The errors are such that our current results are consistent with either summary over the range we can check, and we conclude that this spread represents well the uncertainty in current knowledge.

The addition to the perturbation series that we have made clearly extends the density range over which our knowledge of the hard-core, ground-state energy is reliable to higher densities than was previously possible. In addition, we now have good information for the Fermion fluid energy resulting from weak to moderately strong repulsive square-well interactions over quite a wide range of densities.

[1] G. A. Baker, Jr., M. de Llano, and J. Pineda, Phys. Rev. B **24**, 6304 (1981).
[2] G. A. Baker, Jr., M. de Llano, M. Fortes, L. P. Benofy, S. Peltier, and A. Plastino, Notas Fís. **5**, 47 (1982).
[3] G. A. Baker, Jr., L. P. Benofy, M. Fortes, M. de Llano, S. M. Peltier, and A. Plastino, Phys. Rev. A **26**, 3575 (1982).
[4] G. A. Baker, Jr., G. Gutiérrez, and M. de Llano, Ann. Phys. (N.Y.) **153**, 283 (1984).
[5] G. A. Baker, Jr., M. Fortes, and M. de Llano, in *Recent Progress in Many-Body Theories*, edited by H. Kümmel and M. L. Ristig (Springer-Verlag, Berlin, 1984), p. 351.
[6] G. Gutiérrez, M. de Llano, and W. C. Stwalley, Phys. Rev. B **29**, 5211 (1984).
[7] E. Buendía, R. Guardiola, and M. de Llano, Phys. Rev. A **30**, 941 (1984).
[8] G. A. Baker, Jr., An. Fís. **81**, 65 (1985).
[9] L. P. Benofy, An. Fís. **81**, 67 (1985).
[10] E. Buendía and R. Guardiola, An. Fís. **81**, 70 (1985).
[11] G. A. Baker, Jr., L. P. Benofy, M. de Llano, and M. Fortes, Phys. Rev. C **34**, 678 (1986).
[12] L. P. Benofy, E. Buendía, M. de Llano, and R. Guardiola, Phys. Rev. A **33**, 3749 (1986).
[13] V. C. Aguilera-Navarro, M. de Llano, R. Guardiola, C. Keller, M. Fortes, and M. Popovic, Phys. Rev. A **35**, 3901 (1986).
[14] V. C. Aguilera-Navarro, G. A. Baker, Jr., L. P. Benofy, M. Fortes, and M. de Llano, Phys. Rev. A **36**, 4338 (1987).
[15] V. C. Aguilera-Navarro, R. Guardiola, M. de Llano, and M. A. Solis, Phys. Rev. Lett. **59**, 2322 (1987).
[16] M. de Llano, C. Keller, and V. C. Aguilera-Navarro, J.

Phys. A **21**, 715 (1988).
[17] V. C. Aguilera-Navarro, M. de Llano, C. Keller, and S. Ren, Nucl. Phys. B (Proc. Suppl.) **5A**, 309 (1988).
[18] G. A. Baker, Jr., L. P. Benofy, and M. Fortes, Phys. Rev. C **38**, 329 (1988).
[19] M. de Llano, C. Keller, S. Z. Ren, E. Buendía, and R. Guardiola, Phys. Rev. B **40**, 11 070 (1989).
[20] D. A. McQuarrie, *Statistical Mechanics* (Harper and Row, New York, 1976), Chap. 13; M. H. Kalos, D. Levesque, and L. Verlet, Phys. Rev. A **9**, 2178 (1974).
[21] G. S. Cargill III, in *Solid State Physics,* edited by H. Ehrenreich, F. Seitz, and D. Turnbull (Academic, New York, 1975), Vol. 30, p. 227.
[22] J. L. Finney, Proc. R. Soc. London, Ser. A **319**, 495 (1970).
[23] K. A. Brueckner, Phys. Rev. **100**, 36 (1955).
[24] K. A. Brueckner and K. S. Masterson, Jr., Phys. Rev. **128**, 2267 (1962).
[25] G. A. Baker, Jr., J. L. Gammel, and B. J. Hill, Phys. Rev. **132**, 1373 (1963).
[26] G. A. Baker, Jr., Rev. Mod. Phys. **43**, 479 (1971).
[27] G. A. Baker, Jr., M. F. Hind, and J. Kahane, Phys. Rev. C **2**, 841 (1970).
[28] D. L. Hunter and G. A. Baker, Jr., Phys. Rev. B **7**, 3346 (1973).